Scaling of avalanche queues in directed dissipative sandpiles

Bosiljka Tadić[1,*] and Vyatcheslav Priezzhev[2,†]

[1]*Jožef Stefan Institute, P.O. Box 3000, 1001 Ljubljana, Slovenia*
[2]*Bogolubov Laboratory of Theoretical Physics, Joint Institute of Nuclear Research, 141980 Dubna, Russia*

(Received 24 February 2000)

Using numerical simulations and analytical methods we study a two-dimensional directed sandpile automaton with nonconservative random defects (concentration c) and varying driving rate r. The automaton is driven only at the top row and driving rate is measured by the number of added particles per time step of avalanche evolution. The probability distribution of duration of elementary avalanches at zero driving rate is exactly given by $P_1(t,c) = t^{-3/2} \exp[t \ln(1-c)]$. For driving rates in the interval $0 < r \leq 1$ the avalanches are queuing one after another, increasing the periods of noninterrupted activity of the automaton. Recognizing the probability P_1 as a distribution of service time of jobs arriving at a server with frequency r, the model represents an example of the class $\langle E,1,GI/\infty,1 \rangle$ server queue in the queue theory. We study scaling properties of the busy period and dissipated energy of sequences of noninterrupted activity. In the limit $c \to 0$ and varying linear system size $L \leq 1/c$ we find that at driving rates $r \leq L^{-1/2}$ the distributions of duration and energy of the avalanche queues are characterized by a multifractal scaling and we determine the corresponding spectral functions. For $L \gg 1/c$ increasing the driving rate somewhat compensates for the energy losses at defects above the line $r \sim \sqrt{c}$. The scaling exponents of the distributions in this region of phase diagram vary approximately linearly with the driving rate. Using properties of recurrent states and the probability theory we determine analytically the exact upper bound of the probability distribution of busy periods. In the case of conservative dynamics $c = 0$ the probability of a continuous flow increases as $F(\infty) \sim r^2$ for small driving rates.

PACS number(s): 05.65.+b, 64.60.Ht, 45.70.Ht, 02.50.Hb

I. INTRODUCTION

In the past decade the sandpile type of cellular automata played a special role in understanding self-organized criticality in nonlinear dynamical systems (for a recent review see Ref. [1]). In sandpile automata the properties of the dynamics, which are essential for the occurrence of self-organized critical states, can be monitored in a direct manner. Apart from the relaxation rules, these are the following properties: type of driving and time-scale separation; conservation law of the dynamics; direction of mass flow; and role of boundaries. In addition, the Abelian nature of the toppling rules in some sandpile automata enabled derivation of certain exact results [2,3], in contrast to other dynamical systems where such calculations are not available. Numerous sandpile models, both deterministic and stochastic [1], are shown to exhibit dynamic critical states in the limit of ''infinitely slow'' driving (i.e., at zero driving rate $r = 0$). In this limit a new avalanche is initiated only after the previous one has stopped, thus the time-scale separation is exactly observed. On the time scale of perturbations, the avalanche evolution is seen as occurring instantly. The existence of the critical states in the case of directed Abelian sandpile automaton at zero driving rate has been proved exactly by Dhar and Ramaswamy [2]. At this point it is interesting to mention that the model studied in Ref. [2] is characterized by local driving and deterministic conservative dynamics. The automaton with conservative stochastic dynamics, on the other hand, has been shown to belong to another universality class [4].

The presence of nonconservative defects in Dhar–Ramaswamy automaton leads to a subcritical behavior [5].

The behavior of driven dynamical systems at finite driving rates ($r > 0$) represents an important subject both for theoretical and practical reasons. A finite driving rate may appear either as a control parameter set from outside, or as a probability distribution originating from another coupled stochastic process. In practice, the systems are driven by an external field, which oscillates with a finite frequency. Examples are Barkhausen noise [6], integrate and fire oscillators [7], granular material in rotating drums [8], etc. Queuing jobs at a server [9], e.g., in teletraffic, is an example where the frequency of arriving jobs is given by a random process.

Theoretically at finite driving rates $r > 0$ the probability that a new avalanche starts before the previous one has stopped increases with increasing r. This obviously leads to different statistics of avalanches, where an avalanche is understood to represent a noninterrupted activity of the system. For large driving rates a continuous flow (an avalanche that never stops) is expected in sandpiles. Similarly, a single spanning cluster may occur in driven disordered systems. Therefore, a time-scale separation becomes less and less apparent with increasing r. In addition, by increasing driving rates, the local driving loses its strict sense. Thus fast driven sandpiles are placed between strictly local driving, where the system is driven at a single (random) site, and global driving, where the same perturbation applies to all sites in the system. The role of the conservation law (conservation of number of grains in the interior of the system) is also expected to be changed at finite driving rates. In the $r \to 0$ limit, locally driven nonconservative systems appear to be subcritical [10], whereas when the driving is global the critical states may appear even if the dynamics is dissipative [11,7]. So far nei-

*Electronic address: Bosiljka.Tadic@ijs.si
†Electronic address: priezzvb@thsun1.jinr.ru

ther an exact theory nor a renormalization-group analysis of fast driven critical systems has been done. A general question concerning the existence of critical states at finite driving rates and universal scaling properties of the system in the limit of large distances and long times remains to be answered.

Recently two numerical simulations elucidated certain important properties of sandpiles at finite driving rates. In a one-dimensional ricepile model Corral and Paczuski [12] have first introduced avalanches for a finite driving rate as noninterrupted periods of activity and have shown that these avalanches diverge at rates $r \gtrsim r_c(L) \sim L^{-0.20}$ for a given L. The rational behind this conclusion is that an ever-running avalanche occurs for driving rates $r \sim 1/\langle t \rangle_0$, where $\langle t \rangle_0 \sim L^{z(2-\tau_t)}$ is the average duration of avalanches in zero driving rate [12]. In another example Barrat, Vespignani, and Zapperi [13] have shown that in a two-dimensional symmetric Abelian sandpile model mixing of time scales at finite driving rates leads to correlations that appear to violate the fluctuation-dissipation theorem.

In this work we study a simple two-dimensional model with strictly directed flow of grains and deterministic toppling rules. We add particles *only at the top row* with driving rate r. The driving rate r is defined as a number of added particles per time step of avalanche evolution. We consider both conservative and nonconservative dynamics. A fraction of sites c are considered to be annealed nonconservative defects. By toppling at a defect site two grains are lost, thus affecting the propagation of avalanche below that site [14]. When $c=0$ the dynamics is strictly conservative. In the $r=0$ limit and $c=0$ the model has been exactly solved by Dhar and Ramaswamy [2]. The critical states were shown to consist of heights $h=0$ and $h=1$ occurring with equal probability $1/2$ at each lattice site. The duration of an avalanche is given by the probability distribution for large t

$$P_1(t) \sim t^{-3/2}. \tag{1}$$

In the presence of nonconservative defects it has been shown [5,15] that the screening of the power-law distribution in Eq. (1) occurs as

$$P_1(t) \sim t^{-3/2} \exp(-t/\xi); \quad \xi \sim 1/c. \tag{2}$$

In this paper we will refer to the distributions in Eqs. (1) and (2) as probability distributions of *elementary* avalanches, to be distinguished from the *combined* avalanches, which occur at finite driving rates and which consist of a series of elementary avalanches. Up to relatively high driving rates $r=1$ the model has the property of successive elementary avalanches run one after the other, in contrast to cases studied in Refs. [12,13], where merging of avalanches may occur at any finite r. After an elementary avalanche is over the system is characterized by statistically unchanged distribution of heights, owing to a weak correlation between the avalanches in the recurrent states. A finite probability of avalanche collision, which accelerates flow of grains, occurs in this model only for $r>1$. Here we restrict the study to the case $r \leq 1$, where the formation of avalanche queues is a dominant phenomenon that determines the scaling properties of the system.

The problem of avalanche queue in our model can be regarded as an example of the server queue [9] of the class $\langle E,1,GI/\infty,1 \rangle$, which is studied as a model in the analysis of various applied problems, e.g., in telecommunications, insurance, etc. These analogies are made clear by noticing that the avalanches of a directed sandpile model have the corresponding terms in the language of the queue theory as follows: (i) elementary avalanche—customer; (ii) duration of elementary avalanche—service time; (iii) driving rate—frequency of arrivals of customers; (iv) number of elementary avalanches coexisting at a given moment of time—number of working servers; (v) duration of a combined avalanche—busy period. The notation $\langle E,1,GI/\infty,1 \rangle$ means that we deal with customers arriving by one and being served by one. The letter E means that the arrival times are generated by a Bernoulli process with the distribution $\text{Prob}(t=k) = p^k(1-p); k = 0,1,2, \ldots; p>0$. The symbol GI/∞ means that the service times are identical independently distributed (i.i.d.) random variables and the infinite number of servers provides a nonrestricted number of customers that can be served simultaneously. Despite much literature devoted to this subject [9], most of papers focus on the distribution of q_n, the number of working servers at a given moment of time. The importance of the tail behavior of the busy period distribution for fluid queues in telecommunications, generalized processor sharing, and other applications was recently pointed out in Ref. [16]. Here we concentrate on some other properties of the queue: the scaling behavior of the busy period and dissipated energy distribution.

Given the duration of elementary avalanches in Eq. (1), we may conclude that the directed sandpile model for $r \leq 1$ represents a special case of the queue theory with the power-law distribution of the service time with the exponent $\nu = 3/2 - 1 = 1/2$. This implies that the average service time per customer diverges $\langle t \rangle \to \infty$. In practice, service times are restricted to finite values, which correspond to the power-law distribution with $1 < \nu < 2$ [16]. This may explain why the queue with the distribution of the type given in Eq. (1) has not been studied so far. In our model a finite average duration of elementary avalanches $\langle t \rangle < \infty$ is achieved in two cases: (a) In the case of distribution in Eq. (1) when the system size L is finite, hence the distribution is truncated at $t=L$; (b) In the case of finite dissipation $c>0$, where the distribution in Eq. (2) has a characteristic duration $\xi < \infty$ for all finite c values (see Refs. [5,15] and below).

For a finite L we find a continuous flow phase (F) for low dissipation and large driving rates, and three regions with intermittent behavior of avalanche queues. These are regions with subcritical (S), nonuniversal (N), and multifractal (M) behavior, shown schematically on the phase diagram in Fig. 1. When the length separation $L \gg \xi$ holds, we find a line in the (r,c) plane where loss of particles on defects in the interior of the pile becomes ''compensated'' by fast adding of particles from outside. In the region above the compensation line the avalanche queues exhibit a scaling behavior with the scaling exponents depending on the driving rate: The slopes decrease, whereas the fractal dimensions increase with driving rate. Cutoffs with a stretch-exponential behavior appear. In the limit $c \to 0$ and when the system size $L \ll \xi$ is varied multifractal scaling properties describe the scaled distributions, rather than a simple finite-size scaling.
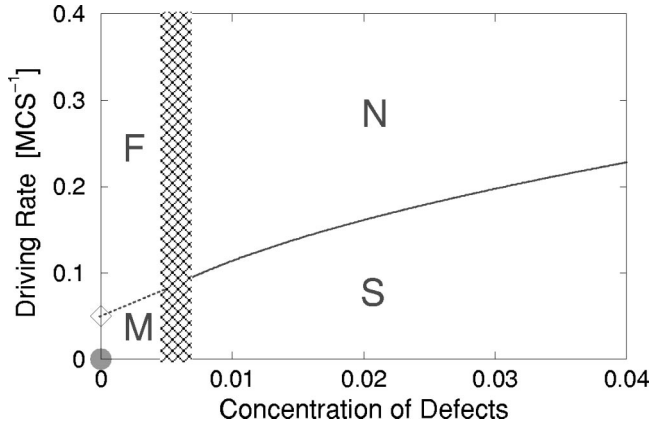
FIG. 1. Schematic phase diagram for a finite system size L. Cross-hatched area represents a crossover region between $\xi \ll L$ (right) and $\xi \gg L$ (left). Regions with distinct behavior of the avalanche queues are shown: subcritical (S), nonuniversal (N), multifractal scaling region (M), and flow phase (F). Solid line represents the compensation line. Transition to the flow phase is marked by ($\diamond$) for $c=0$ and by dotted line for small $c>0$. In the origin ($\bullet$) only single Dhar-Ramaswamy avalanches occur.

In general, the distributions of combined avalanches are characterized by a scaling function of two arguments of the form

$$P(X,r,L_c) \sim X^{-\tau_X} \mathcal{P}(XL_c^{-D_X}, rL_c^{1/2}), \qquad (3)$$

where X represents either duration t or number of topplings [17] n and $L_c \equiv \min\{\xi, L\}$. The corresponding fractal dimensions D_X are defined by

$$\langle X \rangle_{\ell} \sim \ell^{D_X}, \qquad (4)$$

where the average is taken over all combined avalanches of a selected length ℓ measured along the direction of transport.

Using analogy to the queue theory and the properties of the recurrent states we were able to derive an exact upper limit of the distributions of busy periods and to discuss the limit $L \to \infty$. We also derived the expression for the probability of continuous flow in the conservative limit.

The paper is organized as follows: In Sec. II we define the model and consider the case of conservative dynamics by numerical simulations on finite lattice. In Sec. III we present results of simulations in the case of finite concentration of nonconservative defects. In Sec. IV we present details of the analytical results. The paper contains a short summary of the results and discussion in Sec. V.

II. MULTIFRACTAL QUEUES OF DHAR-RAMASWAMY AVALANCHES

The sandpile automaton model introduced by Dhar and Ramaswamy represents an example of a self-organized criticality with exact solution in the limit of zero driving rate [2]. In this section we consider the same model at finite driving rates $0<r \leqslant 1$. The dynamic rules of the model are summarized as follows [2]: We consider a two-dimensional square lattice oriented downward, with a dynamic variable-height $h(i,j)$ associated at each site. Grains are added at the top row only, and mass flow is only down. The toppling at a site
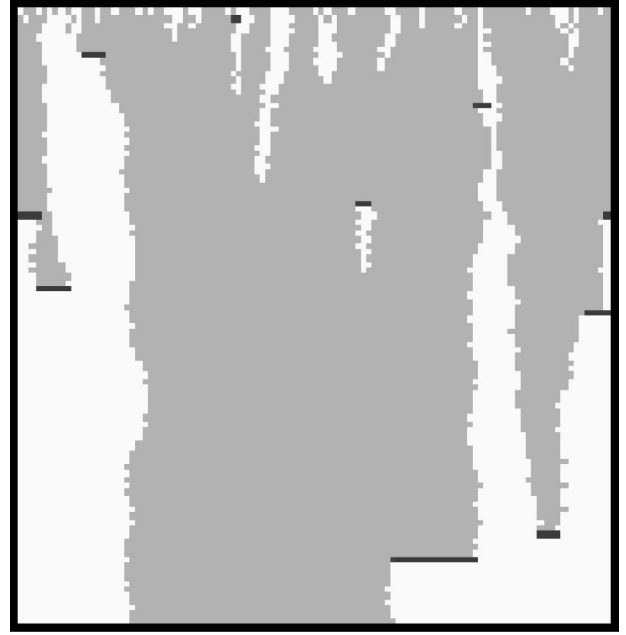
(a)
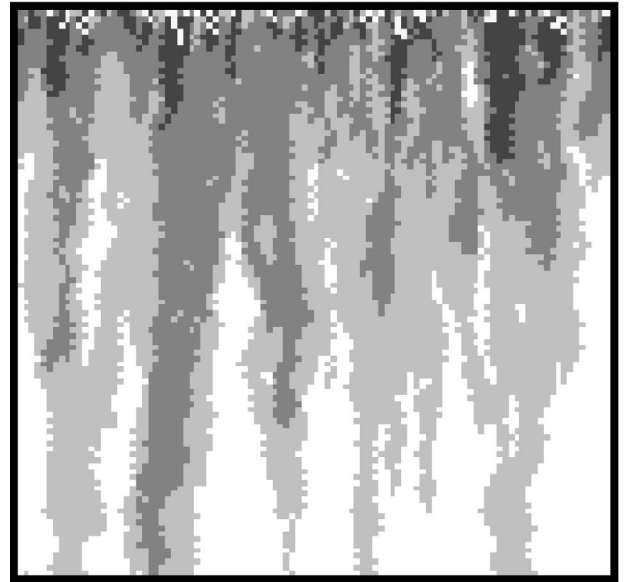
(b)

FIG. 2. (Top) Growth of a combined avalanche in the case of conservative dynamics ($c=0$) for driving rate $r=0.05$ and $L=100$. Nine fronts of active sites (dark) are visible. (Bottom) A complete combined avalanche in the case of dissipative dynamics with $c=0.02$ and driving rate $r=0.5$. Different shades of gray correspond to distinct toppling waves.

(i,j) occurs deterministically whenever $h(i,j) \geqslant h_c=2$, and two grains are transferred downward, i.e.,

$$h(i,j) \to h(i,j)-2; \quad h(i+1,j_{\pm}) \to h(i+1,j_{\pm})+1, \quad (5)$$

where $(i+1,j_{\pm})$ represents two downward neighboring sites to the site (i,j).

The probability distribution of duration of avalanches in zero driving rate $P_1(t) \sim t^{-\tau_t^0} \mathcal{P}(tL^{-1})$ with $\tau_t^0 = 3/2$ given in Eq. (1) becomes exact at large t [2]. In addition the dynamic exponent $z^0=1$. This implies that the average duration $\langle t \rangle_0$
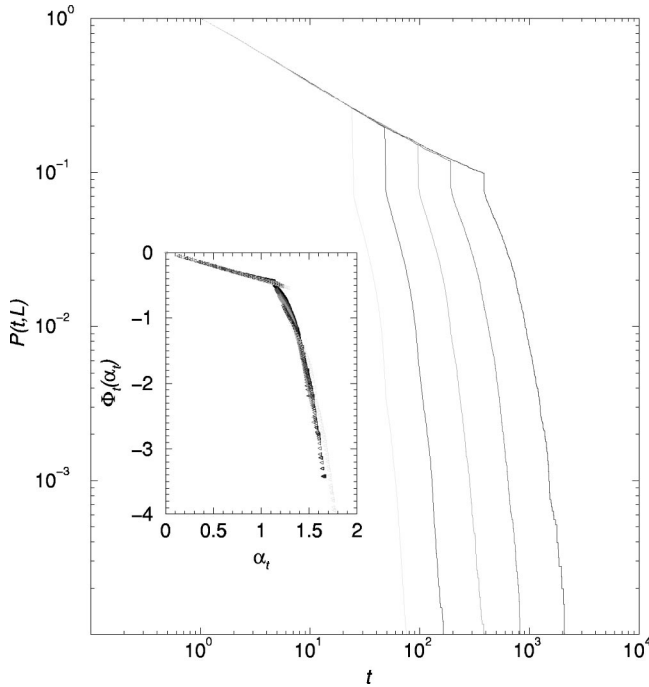
FIG. 3. Double logarithmic plot of the integrated probability distribution of duration (busy periods) $P(t,L)$ of queues of Dhar–Ramaswamy avalanches vs duration t, measured in Monte Carlo steps (MCS's). Fixed driving rate $r=0.05$ and various lattice sizes $L=24$, 48, 96, 192, and 384 are used. (Inset) Multifractal spectral function $\Phi_t(\alpha_t)$ vs α_t obtained from the data in main figure according to Eq. (6) using $X_0=1$, $L_0=2$.

$\sim L^{1/2}\rightarrow\infty$. Similarly, the area s enclosed by the boundary of an avalanche is given by the distribution $D(s,L)$ $\sim s^{-\tau_s^0}\mathcal{D}(sL^{-D_s^0})$, where $\tau_s^0=4/3$ and the fractal dimension $D_s^0=3/2$. Note that the number of toppled grains at each active site is two, then the distribution of the number of toppled grains within an avalanche $D(n)$ is described by the same exponents, i.e., $\tau_n^0=4/3$ and $D_n^0=3/2$ at zero driving rate.

A finite driving rate $r>0$ is implemented as follows. An avalanche is started from the top and at each step of the avalanche progress a new particle is added with probability r at a random site at first row. We also consider a deterministic addition of particles, i.e., we add a particle at regular intervals Δt. Both approaches lead to the same results when the statistics is high enough. An added particle may trigger a new elementary avalanche before the previous one stops, thus making a pattern of active sites distributed over the lattice. A snapshot of growth of a combined avalanche with marked active sites is shown in Fig. 2 (top). A combined avalanche (avalanche queue) is thus determined by a noninterrupted activity on the lattice and it stops when no more active sites occur. Then a new avalanche is started. It should be noted that when $r>0$ the number of added grains is higher than the number of combined avalanches. Another important remark is that the repeated toppling at a site may occur as soon as $r>0$. This leads to the inequality $\langle n\rangle>\langle s\rangle$, and thus $D_n>D_s$, and $z>1$. The numerical simulations confirm these conclusions (see below). Typically, we consider 2×10^6 combined avalanches at each driving rate and lattice size. Periodic boundary conditions are applied in the perpendicular direction.
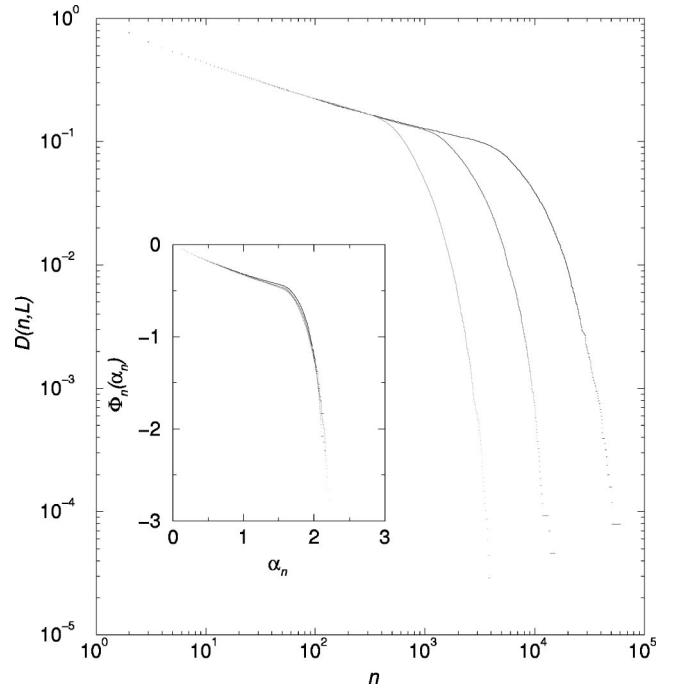

FIG. 4. Same as Fig. 3 but for the integrated distribution of number of topplings (mass) $D(n,L)$ vs mass n (number of grains). Shown are only curves for $L=96$, 192, and 384. (Inset) Spectral function $\Phi_n(\alpha_n)$ vs α_n. $X_0=0.97\pm0.02$, $L_0=2.15\pm0.05$.

In this section we perform numerical simulations for $r>0$ and finite lattice sizes L. The limit $L\rightarrow\infty$ will be discussed in Sec. IV. In Figs. 3 and 4 are shown the integrated probability distributions of duration $P(t'\geq t,L)$ and number of topplings $D(n'\geq n,L)$ for fixed driving rate $r=0.05$ and various lattice sizes L. It should be noted that both slopes and cutoffs of these distributions appear to be different compared to ones of the elementary avalanches. In particular, slopes decrease with r (see a more detailed discussion in Sec. III). For instance at $r=0.05$ we find $\tau_t=0.4$ and $\tau_n=0.3$, in the steep part, and $\tau_t=0.31$ and $\tau_n=0.2$ in the flat part near the cutoff. A cutoff in the probability distribution of durations appears (cf. Fig. 3). The characteristic jump at $t=L$ is related to the conditional probability: an activity lasts longer than L steps only if the preceding avalanches is not shorter than $t=L$. The jump decreases with increasing lattice size. It is interesting that these distributions cannot be scaled according to a simple finite-size scaling (with new exponents), as one may naively expect. Instead, we find that a multifractal scaling applies according to the law

$$P(X,L,r)=\left(\frac{L}{L_0}\right)^{\Phi_X(\alpha_X)}; \quad \alpha_X=\frac{\log(X/X_0)}{\log(L/L_0)}, \quad (6)$$

where, as before, X stands for t or n. The corresponding spectral functions $\Phi_t(\alpha_t)$ and $\Phi_n(\alpha_n)$ are determined numerically for $r=0.05$ and shown in the insets to Figs. 3 and 4, respectively. The spectrum depends on the driving rate. For driving rates close to the line $r\sim L^{-1/2}$ extremely large avalanches may appear and the scaling fits fail. The origin of multifractality in the queues of Dhar–Ramaswamy avalanches can be found in the fact that an unrestricted multiple
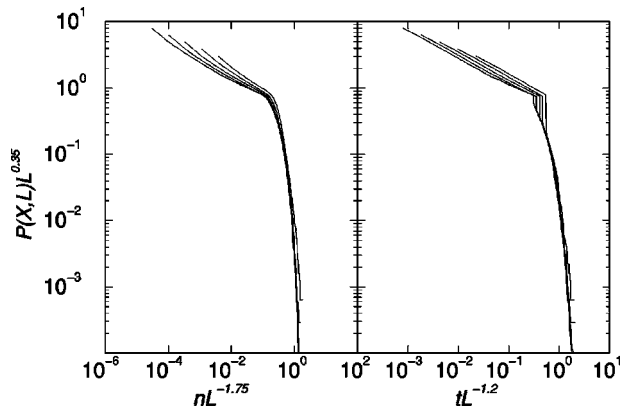
FIG. 5. Attempted finite-size scaling fit of the data from Figs. 3 and 4 for the distribution of avalanche duration (right) and mass (left).

toppling at each site may occur, and that a toppling at a given site releases a local avalanche which propagates from that site downward.

For comparison we show how a finite-size scaling fit of the data fails. In Fig. 5 we present an attempt of scaling collapse of the data shown in Figs. 3 and 4 above, according to the formula $P(X,L) = L^{-\lambda} \mathcal{P}(XL^{-D_X})$. Note that the best collapse of the tails of distributions are obtained by fixing the fractal dimensions as $D_t = 1.20$ and $D_n = 1.75$, which correspond to α_X at the shoulder of the spectrum $\Phi_t(\alpha_t)$ and $\Phi_n(\alpha_n)$, respectively. Fixing a smaller (larger) value for the fractal dimension leads to systematic shifts of the distribution tails to the right (left) with increasing L. The best fit shown in Fig. 5 is obtained for $\lambda = 0.35$, which satisfies (within numerical accuracy) the scaling relation $\lambda = z(\tau_t - 1) = D_n(\tau_n - 1)$ with $\tau_X - 1$ determined at the flat part of the distribution. However, as Fig. 5 shows, fixing D_X and λ leads to the systematic shifts of the ''horizontal'' part of the distributions to the right with decreasing L. Fixing the exponents independently from the scaling relation results in crossing of the lines for different L values.

For driving rates $r > L^{-1/2}$ an ever-running avalanche may occur, representing a continuous activity on the lattice. The flow phase can be characterized by an average number of topplings per site, which is expected to have a nontrivial L dependence. The probability of occurrence of the flow phase in the limit $L \to \infty$ will be discussed in Sec. IV.

III. NONUNIVERSALITY IN DISSIPATIVE DYNAMICS

In the presence of dissipative defects $c > 0$ the distribution of elementary avalanches, which is given in Eq. (2), appears to have a finite characteristic length $\xi < \infty$. Thus the average duration at zero driving rate is finite $\langle t \rangle_0 < \infty$. Precise value of the average duration is controlled by an external parameter probability of dissipation c, and not by system size L, provided that $L > \xi$. The screening length $\xi \sim 1/c$ was first estimated numerically in Ref. [5]. A more precise analytical expression can be derived (see below and Ref. [15]) as $\xi^{-1} \sim -\ln(1-c)$. Here we perform numerical simulations in the case $L > \xi$ at driving rates $0 < r \leq 1$. In this range of driving rates we expect the role of lattice size in the analysis of Sec. II to be replaced by the characteristic length ξ. In addition,
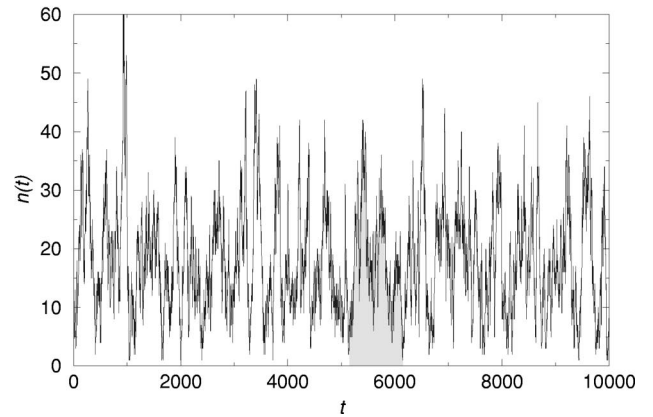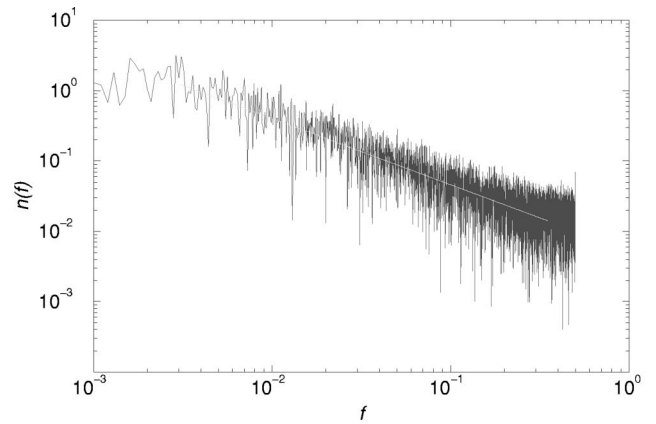

FIG. 6. Sandpile noise $n(t)$—number of active sites at time t, plotted against time t (MCS) (lower panel) and its Fourier spectrum (top panel) for fixed driving rate $r = 0.33$. Dissipation rate $c = 0.01$ and $L = 128$. Shaded area shown in the lower panel is an example of unit signal, corresponding to a combined avalanche.

competition between dissipation and driving rate leads to new phenomena.

In Fig. 2 (bottom) an example of a combined avalanche is shown for $c = 0.02$ and driving rate $r = 0.5$. It is remarkable that the number of topplings per site decreases with distance from the top. Intermittency of the dynamics as well as the occurrence of the long-range correlations can be seen by direct examination of the recorded activity of the system $n(t)$ at each time step. For the server queue the quantity $n(t)$ is interesting as the measure of the energy, which is dissipated by the server at a given moment of time t. In Fig. 6 we show an example of the recorded signal for a certain choice of parameters r, c, and L corresponding to the region (N) of the phase diagram (cf. Fig. 1). A combined avalanche on this recording is represented by a set of peaks between two consecutive drops of the signal to the base line. The Fourier spectrum of the signal (shown on top panel in Fig. 6) exhibits a power-law behavior. The slope $\varphi \approx 0.9$ weakly increases with driving rate r.

The scaling properties of the distributions of avalanche queues depend on the mutual ratio of the driving and dissipation rates. In particular, the scaling function in Eq. (3) exhibits a nontrivial dependence on both arguments $x \equiv t\xi^{-1}$ and $y \equiv r\xi^{1/2}$. [Another suitable choice of variables would be $(tc, rt^{1/2})$.] In Fig. 7 we show the distribution of the avalanche mass (dissipated energy) n for fixed $c = 0.01$
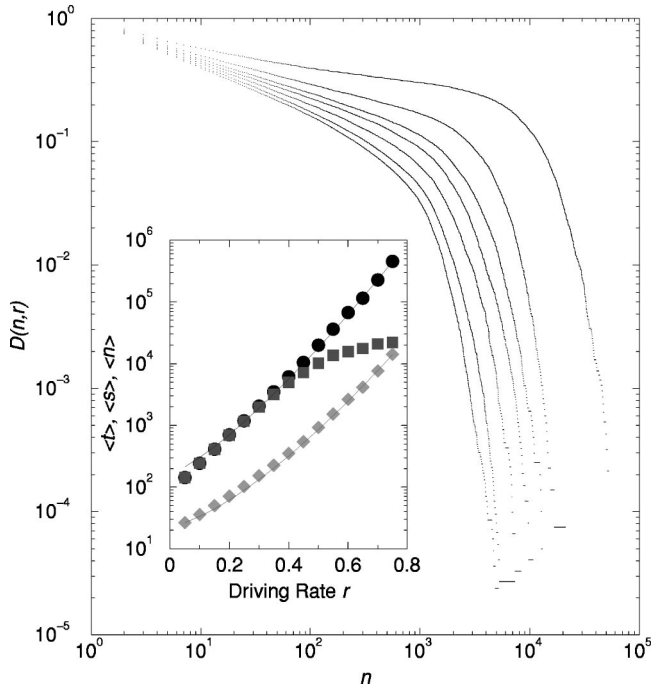
FIG. 7. Distribution of avalanche mass $D(n,r)$ vs mass n (number of grains) shown in double logarithmic scale for fixed dissipation rate $c=0.01$ and $L=192$ and for various driving rates r $=0.021$, 0.041, 0.083, 0.125, 0.166, 0.25, and 0.33 (left to right). (Inset) Average mass (top), area (middle), and duration (bottom) of combined avalanches plotted against driving rate (MCS^{-1}) for fixed $c=0.01$ and $L=192$. At each point average is taken over 2×10^6 combined avalanches. Fitting curves: $\langle n\rangle=167$ $\times\exp(11.4r^{1.28})$, and $\langle t\rangle=23\times\exp(9.6r^{1.42})$.

and various driving rates r. In general, the cutoffs of the distributions increase and slopes decrease with increased driving rates r. More detailed analysis of the slopes shows that for the range of values of driving rates the scaling behavior of the distributions can be described by the scaling exponents which depend on the driving rate. The slopes of various distributions and the corresponding fractal dimensions, which are defined in Eq. (4), are shown against the driving rate in Fig. 8. The dissipation rate is fixed at c $=0.01$. Note that τ_{ℓ} in Fig. 8 represents a slope of the distribution of the largest linear length reached in a combined avalanche. For a range of values of driving rates the scaling exponents decrease and the fractal dimensions increase with r, while the scaling relations between various exponents are found to be satisfied within numerical error bars. The variation of the scaling exponents can be approximated by a linear dependence of r. It is interesting to note that a qualitatively similar behavior, linear variation of the scaling exponents with driving rate, has been measured experimentally in the case of Barkhausen noise in driven disordered ferromagnets [6]. Our present analysis suggests that such behavior can be related to an interplay of driving rate and dissipation at defects, and that it applies more universally. Dependence of the fractal dimensions (and of the slope exponents via scaling relations) of the avalanche queues on driving rate r can be linked to the r dependence of the average length of the queue $\langle N\rangle=1+r\langle t\rangle_0$. It has been shown recently [18] that the fractal spectrum of the series of elementary signals in the case of transit times in the ricepile model varies as a power of the
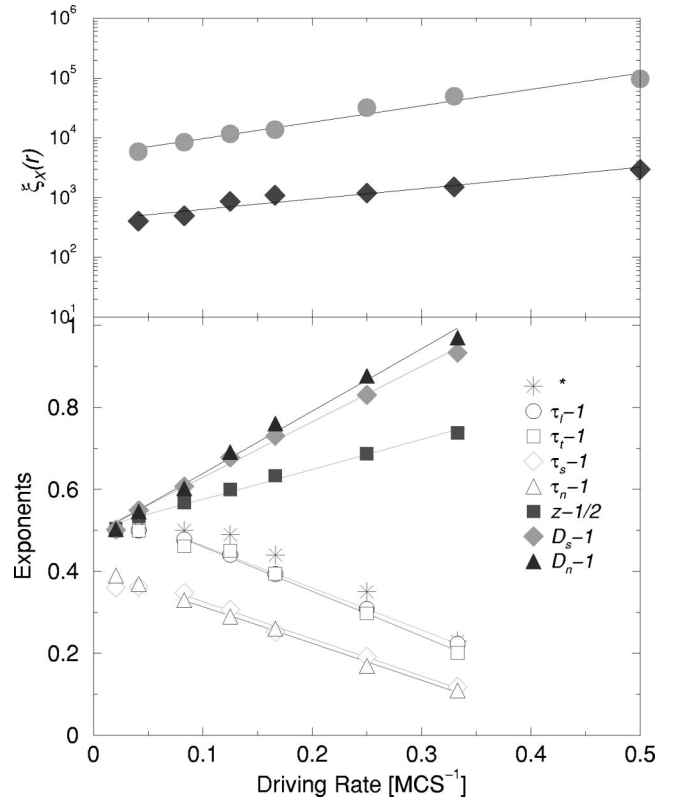

FIG. 8. (Lower panel) Various scaling exponents of the avalanche queues plotted against driving rate for fixed dissipation $c=0.01$ and $L=192$. (*) indicates the products $z(\tau_t-1)\approx D_n(\tau_n-1)\approx D_s(\tau_s-1)\approx 1.1(\tau_{\ell}-1)$. Also shown are linear fits of the data. (Top panel) Amplitudes ξ_n (upper curve) and ξ_t defined in Eq. (7) vs driving rate. (Lines) fit curves satisfying Eq. (8) with B_n $=6.29\pm0.46$ and $B_t=4.5\pm0.51$.

length of series. A precise r dependence of the exponents in the case of avalanche queues requires additional work and will be given elsewhere.

The opposite effects on the exponents are obtained by increasing concentration of defects c at a fixed driving rate. In particular, the slopes of the distributions increase and fractal dimensions decrease with *increasing* concentration of defects in a limited range [19].

An exact expression for the scaling function $\mathcal{P}(x,y)$ in Eq. (3) cannot be guessed. It appears that the cut of the surface $\mathcal{P}(x,y)$ at $r=$const for well balanced values of c and r can be approximated by a stretch-exponential function, so that we have

$$P(X,c,r)=X^{-\tau_X(r)}\exp[-X^{\sigma_X}/\xi_X(r)]. \qquad (7)$$

Here X stands for n or t, and we find $\sigma_n=1.14\pm0.04$ and $\sigma_t=1.28\pm0.06$, for the distribution of energy and duration, respectively. The amplitudes $\xi_X(r)$ can be fitted (see top panel of Fig. 8) by the following function of driving rate r:

$$\xi_X(r)=A_X(c)\exp[rB_X(c)], \qquad (8)$$

for a fixed dissipation rate c.

The observed parameter dependence of the probability distributions is also reflected in the behavior of the average duration and energy of combined avalanches. Notice that the

average duration $\langle t \rangle$ represents the average busy period of a server in the queue theory. Beside the average duration $\langle t \rangle$, we also compute the average values of number of topplings (energy) $\langle n \rangle$ and area $\langle s \rangle$ (total number of distinct sites) affected by the processing of a combined avalanche. These average values are shown versus r in the inset to Fig. 7 for $c = 0.01$. The values $\langle t \rangle$ and $\langle n \rangle$ increase with driving rate faster than an exponential function. Fitting the data in the inset to Fig. 7 we find

$$\langle X \rangle = a_{0X} \exp[a_{1X}(c) r^{\sigma}], \qquad (9)$$

where $X \equiv n, t$ and we estimate $\sigma = 1.2 \pm 0.1$. Note that, in contrast to durations and energies, the average area of an avalanche is bounded by the number of cells in the system $\langle s \rangle \leq L^2$.

As already mentioned above, for a given dissipation rate c and $L \gg \xi$ a driving rate $r_0(c)$ exists such that fast addition of grains compensates the losses in the bulk. In fact along an extremal line

$$r_0(c) \sim \kappa \xi^{-1/2} \approx \kappa \sqrt{c} \qquad (10)$$

the coherence length remains constant. The existence of the compensation line Eq. (10) can be demonstrated by considering sets of data for average durations and energies against driving rate r, obtained for different characteristic length $\xi \sim 1/c$. These data can be scaled according to the following scaling form

$$\langle X \rangle \xi^{-D_X(2-\tau_X)} = \mathcal{G}(r \xi^{z(2-\tau_t)} - \kappa). \qquad (11)$$

The corresponding scaling fits for the two cases $X \equiv t$ and $X \equiv n$ are shown in Fig. 9. Notice that the respective exponents $D_n(2-\tau_n) = 1$ and $z(2-\tau_t) = 1/2$ are exact values, thus leaving only one parameter, namely κ, to be determined by the fitting procedure. This is an advantage of having the exact solution for the elementary avalanches [2]. From the best fit we find $\kappa = 1.14 \pm 0.1$ in the given range of values of c (see caption to Fig. 9). It is evident from Fig. 9 that the scaling function defined in Eq. (11) increases faster than an exponential.

In the simulations a continuous flow may occur in the case of dissipative dynamics at finite lattice size L when the driving rate is increased. However, with increased system size L the behavior is different from that in the case of conservative dynamics discussed above. From the numerical simulations alone we cannot distinguish if the affected area of a continuous avalanche diverges with the system size $L \to \infty$, or it remains finite for the range of driving rates considered here. We will also discuss large L limit in Sec. IV.

We have restricted our analysis to the case where the degree of dissipation is such that $\xi \ll L$. For $c \to 0$, however, we have $\xi \to \infty$, thus the role of L and ξ is interchanged at some finite L. In the reverse limit when $L \ll \xi$ the behavior is expected to be similar to the case of conservative dynamics at finite L, studied in Sec. II.
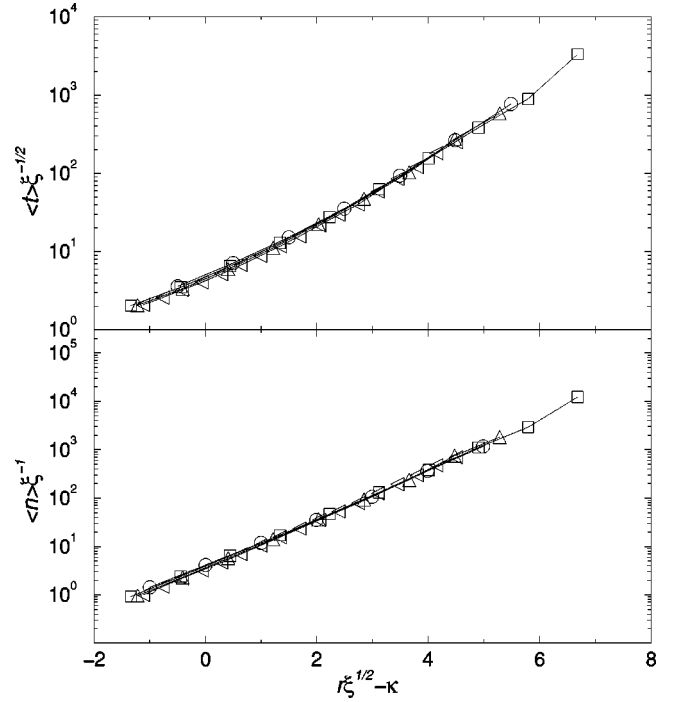

FIG. 9. Finite-size scaling plot of the average duration $\langle t \rangle$ (top) and mass $\langle n \rangle$ (bottom) according to Eq. (11). Data are taken for values of $c = 0.01$, 0.0125, 0.015, and 0.02 such that $\xi < L = 192$ is satisfied. Note that the exponents are exact and the fitted value $\kappa = 1.14$ within numerical error bars.

IV. ANALYTICAL RESULTS

We start the analytical description of the model with the assumption that individual avalanches, which form a combined avalanche, are statistically independent. By the definition of the model, each toppling in a single avalanche occurs later than those in the previous avalanches, so that the individual avalanches never intersect in the space-time points. Nevertheless, the next avalanche is sensitive to the configuration of occupation numbers left by the previous avalanches. In this way the individual avalanches are dependent on preceding avalanches. On the other hand, it is known from Abelian properties of the directed sandpile model [2], that the recurrent state is characterized by the independent distribution of occupation numbers zero and one at each site. Hence, one can expect that this property of recurrent state provides independent distribution of single avalanches at least for asymptotically large systems. This assumption allows us to consider the process of driving the directed sandpile automaton as a sequence of i.i.d. events. Another important consequence of the statistical independence is that stops of combined avalanches can be considered as recurrent events, i.e., the probability of two successive stops $\mathrm{Prob}(t_1, t_2)$ at the moments t_1 and $t_1 + t_2$ is given by the product $\mathrm{Prob}(t_1)\mathrm{Prob}(t_2)$.

We consider the probability distribution $F(t)$ that a combined avalanche starting at the moment $t = 0$ stops *for the first time* at the discrete moment t. This means that $F(t)$ is the probability that the stop of all preceding elementary avalanches occurs until the moment t. Thus, $F(t)$ coincides with the probability distribution of duration of combined avalanches when an ensemble of events is considered. Along

with $F(t)$, it is useful to consider the function $U(t)$, which is defined as the probability that all preceding single avalanches stop to the moment t *regardless* of how many stops of combined avalanches occurred before t. Noting that stops of combined avalanches are recurrent events, we can write for $F(t)$ and $U(t)$ the following identity [20]:

$$U(t)=F(1)U(t-1)+F(2)U(t-2)+\cdots+F(t)U(0), \quad (12)$$

where it is convenient to put $F(0)=0$ and $U(0)=1$. For the generating functions defined by

$$u(s)=\sum_{t=0}^{\infty} s^t U(t) \quad (13)$$

and

$$f(s)=\sum_{t=1}^{\infty} s^t F(t) \quad (14)$$

one easily gets from Eq. (12) the known equation of the theory of recurrent events [20]

$$f(s)=\frac{u(s)-1}{u(s)}. \quad (15)$$

The total probability that a combined avalanche ever stops is given by $f(1)$. Therefore, the probability that a combined avalanche never stops, i.e., the probability of a continuous flow, which is given by

$$F(\infty)=1-f(1), \quad (16)$$

does not vanish if $u(1)$ in Eq. (15) is finite $u(1)<\infty$.

A. Case $c=0$

In the case of conservative dynamics ($c=0$) the probability distribution of durations of elementary avalanches is given by Eq. (1). Then we can estimate the probability $U(t)$ as follows. Let $\Delta t \equiv 1/r$ be the average time interval between addition of successive particles to the first row. The probability $\mathrm{Prob}(x \leqslant t)$ that a single avalanche has a duration less than t is

$$\mathrm{Prob}(x \leqslant t) \sim 1 - \frac{b}{t^{1/2}} \quad (17)$$

for large t, where b is a constant of the order unity when L is large. Then for times $t \gg \Delta t$ we have

$$U(t) \sim \left(1-\frac{b}{t^{1/2}}\right)\left(1-\frac{b}{(t-\Delta t)^{1/2}}\right)\cdots\left(1-\frac{b}{(\Delta t)^{1/2}}\right). \quad (18)$$

Introducing $k=t/\Delta t$ we can write Eq. (18) as the sum

$$\ln U(t)=\sum_{n=1}^{k} \ln\left(1-\frac{b}{(n\Delta t)^{1/2}}\right)\leqslant -\frac{k^{1/2}}{(\Delta t)^{1/2}}. \quad (19)$$

Approximating the sum by an integral leads to

$$U(t) \sim \left(\frac{\sqrt{rt}-b\sqrt{r}}{1-b\sqrt{r}}\right)^{-b^2 r} \exp[-2b(r\sqrt{t}-\sqrt{r})] \quad (20)$$

for $t \gg 1$ and $0 < r \leqslant 1$. For the infinite lattice there exists a constant c_2 such that

$$u(1) \leqslant c_2 \sum_{t=0}^{\infty} \exp(-r\sqrt{t}) < \infty. \quad (21)$$

Therefore, we can find that for all finite driving rates $r>0$ there is a nonzero probability of continuous flow. In particular, the sum in Eq. (21) diverges at small r as

$$u(1) \sim \frac{1}{r^2} \quad (22)$$

leading to the probability of stop $f(1) \sim 1 - 2r^2 b^2$, which decreases from unity as soon as a finite driving rate is applied. Then the probability of continuous flow Eq. (16) increases from zero by the same amount, i.e.,

$$F(\infty) \sim r^2, r \to 0. \quad (23)$$

For large r we expect that

$$1-F(\infty) \sim \exp(-r). \quad (24)$$

If the size of the system is finite ($L<\infty$) the probability of stops $U(t)$ is bounded from *above* by a finite value

$$U(t) \leqslant (rL)^{-b^2 r/2} \exp(-2brL^{1/2}), \quad (25)$$

which follows from Eq. (20) taking only the dominant t behavior for $t=L \gg 1$.

B. Case $c>0$

In the case of finite dissipation rate $c>0$ the dissipation leads to a finite characteristic length ξ in the distribution of elementary avalanches in Eq. (2). This can be easily demonstrated using mean-field arguments [21] in reaction-diffusion systems. Let us suppose that at each site of the lattice one of species A or B is living. These species represent two possible states of the original model: A corresponds to the empty site, B to the occupied site. Due to the external driving force, new particles ϕ are added to the first row of the lattice at rate r. The propagation of particles can be described by the following rules:

$$A+\phi \to B, \quad B+\phi \to A+2\phi. \quad (26)$$
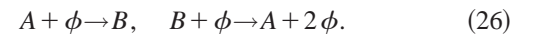
The kinetic equations corresponding to this scheme of ''chemical'' reactions are

$$\dot{n}_A(\ell)=n_\phi(\ell)[n_B(\ell)-n_A(\ell)], \quad (27)$$

$$\dot{n}_B(\ell)=n_\phi(\ell)[n_A(\ell)-n_B(\ell)], \quad (28)$$

$$\dot{n}_\phi(\ell)=-n_\phi(\ell)+2n_\phi(\ell-1)n_B(\ell)(1-c), \quad (29)$$

where $n_A(\ell)$, $n_B(\ell)$, and $n_\phi(\ell)$ are concentrations of species A, B, and ϕ, respectively, at the ℓth row. In the steady

state we have $\dot{n}_A = \dot{n}_B = \dot{n}_\phi = 0$ and Eqs. (27)–(29) lead to the simple conditions for the concentrations $n_A = n_B = 1/2$ and [22]

$$n_\phi(\ell) = r(1-c)^\ell. \tag{30}$$

For $c > 0$, the density of particles ϕ, and hence the number of topplings in an avalanche, decay exponentially with the distance ℓ from the top as $n_\phi(\ell) = r \exp(-\ell/\xi)$. This implies that the characteristic length of the avalanche is $\xi^{-1} \sim -\ln(1-c) \sim c$. Therefore the above results, in particular Eq. (25), obtained for the case of finite lattices L and $c = 0$ apply also for the case $c > 0$ by the substitution $L \to L_c$ with

$$L_c = \min\{\xi, L\}. \tag{31}$$

C. Bounds for the busy time

If the combined avalanches are finite (i.e., there is no continuous flow), we can estimate their average duration using the known theorem from the theory of recurrent events (Ref. [20], Ch. XIII, Theorem 3). According to this theorem, the inverse average time of combined avalanches $\langle t \rangle^{-1}$ coincides with the limit of the sequence $U(t)$ when $t \to \infty$. Using the bound for $U(t)$ given by Eq. (25) we get

$$\langle t \rangle \geq (rL)^{b^2 r/2} \exp(2brL^{1/2}). \tag{32}$$

The true asymptotics of $\langle t \rangle$ possibly contains an additional prefactor $L^{1/2}$ as in the case for $r = 0$. Notice that numerically the average duration as a function of r (cf. inset to Fig. 7) increases faster than the exponential, which agrees with Eq. (32).

The combination $rL^{1/2}$ appears as a characteristic parameter determining the duration of combined avalanches. Thus, for $\xi < L$ it follows from Eqs. (32) and (30) that the coherence length remains constant if r varies with c as $r \sim \sqrt{c}$, i.e., the increasing driving rate compensates the dissipation.

Another interesting feature of the probability distributions at finite driving rates is the occurrence of stretch-exponential cutoffs in both dissipative and nondissipative cases (cf. Figs. 3, 4, and 7). Indeed, we can see from Eq. (12) that $U(t) > F(t)$ for all finite t. Therefore, for the nondissipative case we have an exponential decay of combined avalanches

$$P(t) \sim F(t) < (rt)^{-b^2 r/2} \exp(-2br\sqrt{t}) \tag{33}$$

in the thermodynamic limit $L \to \infty$, which follows directly from Eq. (20) for large t.

For finite lattice sizes L or finite dissipation $c > 0$ the function $U(t)$ is bounded from above by a constant given in Eq. (25) with L replaced by L_c. In this case we can find the origin of an exponential cutoff in the following way. Consider an enveloping process that corresponds to propagation of the front of the combined avalanches. Duration of an elementary avalanche starting at t_{i0} is a simple linear function of time $t_i = t - t_{i0}$. The enveloping process consists of those topplings which occur at the maximal distance from the time axis at each moment of time t. The position x of the front is an one-dimensional random walk confined to the interval $[0,\xi]$. Starting from $x = 0$, the walk performs a step ahead with some probability, and a step back, the length of which is

a random variable. The combined avalanche stops if the random walk returns to the origin where it is trapped. The probability of the return to the origin from an arbitrary position x is not smaller than $U(\xi)$, where

$$U(\xi) = (r\xi)^{-b^2 r/2} \exp(-2br\xi^{1/2}), \tag{34}$$

and $\xi \sim 1/c$ as above. The survival time t of the random walk under consideration does not exceed the period of successful tests in the Bernoulli scheme with the probability of "success" $1 - U(\xi)$. The period of tests in the Bernoulli process has the geometrical distribution

$$\text{Prob}(x = t) = [1 - U(\xi)]^t U(\xi). \tag{35}$$

Hence, the time distribution for combined avalanches is bounded from above by the exponential function in Eq. (35). Using Eq. (34), we obtain

$$P(t) \sim F(t) < A(1 - U(\xi))^t \sim A \exp[-tU(\xi)], \tag{36}$$

where A is a constant and $U(\xi)$ is given by Eq. (34). Note that this expression represents an upper bound of the distribution of busy periods in Eq. (7). Therefore $1/U(\xi)$ plays the role of an effective correlation length at finite r, in a qualitative agreement with the numerical data and Eq. (8) of Sec. III.

V. CONCLUSIONS AND DISCUSSION

We have shown that a finite driving rate r is a relevant perturbation, which alters self-organized critical states in the directed sandpile automata. In the case of conservative dynamics r couples to $\langle t \rangle_0 \sim L^{1/2}$, thus leading to enhanced effects when the length scale is increased to $L \to \infty$. A continuous flow eventually occurs, in which critical long-range correlations are destroyed. On a finite length scale, $L_c = \min\{\xi, L\} < \infty$ either due to finite screening length ξ or finite system size L, the critical states occur with qualitatively new correlation properties, which is manifested in: (i) a multifractal scaling of combined avalanches when $L \ll \xi$, and (ii) occurrence of compensation between driving and dissipation along a line $r_0(c) \sim \xi^{-1/2} \sim \sqrt{c}$, when $L \gg \xi$. How precisely the effective coherence length $\xi_{\text{eff}}(r)$ of combined avalanches increases with driving rate depends on details of the relaxation process and grain addition. In the case of a finite input current at each site of the system, we find a finite toppling rate at all scales, $n_\phi(\ell) \sim r/c$, compatible with $\xi_{\text{eff}}(r) \to \infty$. However, if grains are added only at the top, the correlation length increases exponentially with r in the range $0 < r \leq 1$, but remains finite presumably up to large driving rates. Here we restricted the discussion to the case $r \leq 1$, where queues of Dhar–Ramaswamy avalanches occur. Avalanche queuing for this range of driving rates is peculiar to our model, due to strictly local critical height rule and the directed transport. In the ricepile and in the symmetric Abelian models [12,13] a perfect queuing is prevented by the collision of avalanches, which occurs at any finite $r > 0$. Owing to the exact solution for behavior of elementary avalanches [2], we were able to study properties of the queue in detail. In particular, we find that an average busy period is bounded from below by an exponential function

$\langle t \rangle \gtrsim (rL)^{b^2 r/2} \exp(2brL^{1/2})$. The avalanche queue can be regarded as a multifractal set, in which the average length is regulated by the driving rate as $\langle N \rangle = 1 + rL^{1/2}$. There are no waiting times for elementary avalanches, therefore our model corresponds to the realization known in the queue theory as ''infinite number of servers.'' Hence, the average number of jobs q_n that can be served in parallel is unlimited. It should be stressed that our cellular automaton represents a new example in the queue theory in which queuing jobs are distributed according to a power-law distribution with the exponent $\nu < 2$ and average duration of jobs is limited by a control parameter $L_c = \min\{\xi, L\}$. We hope that more practical examples of this class can be found. We also believe that the study of the scaling properties of the queues, as we have done in this work, adds a new aspect which has not been considered so far in the queue theory. The observed nonuniversal scaling properties of avalanche queues can be related to variation of the average length of the queue with driving rate. The scaling exponents are found to vary approximately linearly with the driving rate r. A similar r dependence was observed experimentally in other driven disordered systems, and seems to apply more generally.

A continuous activity on the lattice, corresponding to a flow phase occurs for $r \geq L^{-1/2}$ in the case of conservative dynamics. On an infinite lattice $L \to \infty$ probability of continuous flow increases from zero as $F(\infty) \sim 2b^2 r^2$, whereas probability of an intermittent avalanche-like flow decreases from unity with the same rate $f(1) \sim 1 - 2b^2 r^2$. For the case of dissipative dynamics $c > 0$ an effective coherence length increases with r for $1/c < L \to \infty$. Our results suggest that the probability $f(1)$ remains finite even at high driving rates. In the limit $L \to \infty$ the compensation line extends to the point $c \to 0$, $r \to 0$. For the range of driving rates studied in this work we expect that the transport properties of grains in this model remain unchanged (looked at the time scale of avalanche propagation), compared to the transport at zero driving rate [23]. Collision of avalanches, which occurs first at rates $r > 1$, may accelerate the grain transport possibly resulting in a new scaling behavior of the distribution of transit times. Notice that due to local critical height rules and deterministic topplings the depth of the active zone (defined in Ref. [12]) does not change in the flow phase of our model.

The analytical results in Sec. IV are derived assuming that elementary avalanches may be considered as independent events. We checked by computing numerically the correlation function between events in a queue for finite L where rather weak correlations occur. The correlations increase with the ''distance'' τ between avalanches as τ^η, where $\eta = 0.05 \pm 0.01$ with statistical error bars.

[1] D. Dhar, Physica A **263**, 4 (1999).

[2] D. Dhar and R. Ramaswamy, Phys. Rev. Lett. **63**, 1659 (1989).

[3] See Ref. [1] for more exact results.

[4] B. Tadić and D. Dhar, Phys. Rev. Lett. **79**, 1519 (1997).

[5] B. Tadić, U. Nowak, K. D. Usadel, R. Ramaswamy, and S. Padlewski, Phys. Rev. A **45**, 8536 (1992).

[6] G. Bertotti, G. Durin, and A. Magni, J. Appl. Phys. **75**, 5490 (1994); G. Durin and A. Magni, in *Fractal Reviews of the Natural and Applied Sciences*, edited by M. Novak (Chapman & Hall, London, 1995).

[7] A. Corral, C. J. Pérez, A. Díaz-Guilera, and A. Arenas, Phys. Rev. Lett. **74**, 118 (1995).

[8] H. M. Jaeger, C.-Heng Liu, and S. R. Nagel, Phys. Rev. Lett. **62**, 40 (1989); M. Bretz, J. B. Cunningham, P. L. Kurczynski, and F. Nori, *ibid.* **69**, 2431 (1992).

[9] A. A. Borovkov, *Veroyatnostnie Processi v Teorii Massovovo Obsluzhivaniya* (Nauka, Moscow, 1972); J. W. Cohen, *The Single Server Queue*, 2nd ed. (North-Holland, Amsterdam, 1982).

[10] See, e.g., Ref. [5] and B. Tadić and R. Ramaswamy, Phys. Rev. E **54**, 3157 (1996).

[11] See Ref. [7] and S. S. Manna, L. Kiss, and J. Kértez, J. Stat. Phys. **61**, 923 (1990); K. Christensen and Z. Olami, Phys. Rev. A **46**, 1829 (1992); S. S. Manna (unpublished).

[12] A. Corral and M. Paczuski, Phys. Rev. Lett. **83**, 572 (1999).

[13] A. Barrat, A. Vespignani, and S. Zapperi, e-print cond-mat/9903269.

[14] This implementation correspond to site defects. A bond type of defects is expected to have qualitatively similar effects [A. Povolotsky (unpublished)].

[15] J. Theiler, Phys. Rev. E **47**, 733 (1993).

[16] A. P. Zwart, Eindhoven University of Technology, Memorandum COSOR 99-12, 1999 (unpublished).

[17] Number of topplings n occurring during an avalanche (also called avalanche mass) in this model is proportional to the energy dissipated in the avalanche. Here we use all three terms equally.

[18] R. Pastor-Satorras, Phys. Rev. E **56**, 5284 (1997).

[19] Somewhat similar effects of disorder have been observed in disordered ferromagnets at finite driving rates [B. Tadić, Phys. Rev. Lett. **77**, 3843 (1996)].

[20] W. Feller, *An Introduction to Probability Theory and Its Applications*, 2nd ed. (Wiley, New York, 1971).

[21] E. V. Ivashkevich and V. B. Priezzhev, Physica A **254**, 97 (1998).

[22] Note that the behavior is different in the case of addition of particles at *each site* on the lattice, when we have a constant number of topplings at all distances $n_\phi(\ell) = (r/c)[1 + (1-c)^{\ell-1}]$ controlled by the ratio r/c.

[23] B. Tadić (unpublished).